Radiating element of GEODA-SARAS

José Manuel Inclán Alonso, Álvaro Noval Sánchez de Toca, Javier García-Gasco Trujillo, José Manuel Fernández González, Manuel Sierra Pérez.

{chema, anoval, jtrujillo, jmfdez, m.sierra.perez}@gr.ssr.upm.es
Grupo de Radiación ,Dpto. de Señales, Sistemas y Radiocomunicaciones Universidad Politécnica de Madrid Avda. Complutense, 30. 28040 Madrid. España.

.

Abstract- **This document shows the design of the radiating element of the conformal adaptive antenna of multiple planar arrays GEODA-SARAS. Operating from 2.05 to 2.3 GHz in the S-band with dual circular polarization in Tx and Rx, it is possible to track and communicate with several satellites because of its adaptive beam. The antenna is based on a set of similar triangular arrays which are divided in sub-arrays of five elements called cells.**

I. INTRODUCTION

The GEODA-SARAS is an evolution of GEODA [1] and GEODA-GRUA [2]. This antenna consists of 6 planar arrays of 45 elements grouped in 9 cells. The antenna is able to transmit in selectable circular polarization and able to receive in both circular polarizations simultaneously. The mechanical structure of the antenna is shown in Fig. 1.

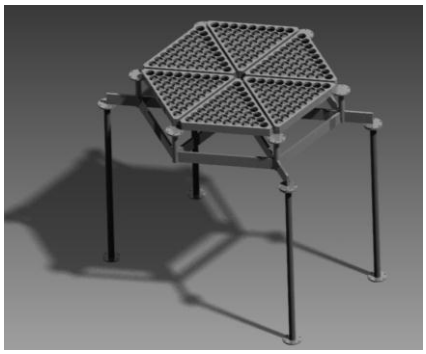

Fig. 1 Mechanical structure of the antenna

Each of the cells must have the necessary circuits to select the polarization and to steer the antenna changing the phase of each element with commercial phase shifters. Moreover every element has a T/R module with an amplification chain and diplexer filters to separate Tx from Rx. A printed coupler is also used in every element for calibrating the antenna.

The layout of the RF circuits for one cell is presented in Fig. 2.

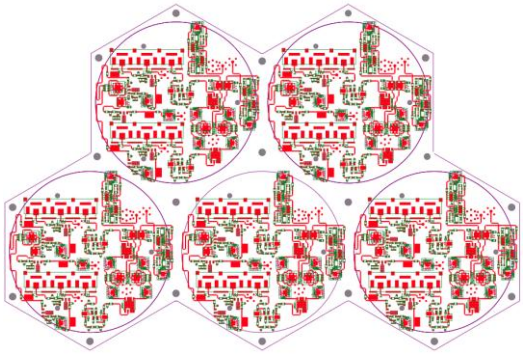

Fig. 2 Cell RF Layout

II. RADIATING ELEMENT STRUCTURE

The radiant element consists of a dual resonant circular patch that allows obtaining a wide diagram with dual linear polarization among the design frequency band. Previous experience indicates that this structure is perfectly feasible with an acceptable result in terms of polarization, input impedance and radiation pattern.

One typical drawback of the printed structures is the strong coupling between closed elements, which significantly affects the input impedance when varying the pointing direction. In this sense it is convenient to work with patches included in metallic cavities to reduce this coupling effect. In Fig. 3 (a) and (b) is shown the dual patch inside the cavity.

Another typical problem is the coupling between both linear resonant modes. In theory the two orthogonal modes in the patch are isolated and no coupling appears between them, but there is some coupling associated to the vertical feeding poles of the patch. This makes the design process more complicated since a good matching and also a low coupling between polarizations are desired. To reduce the coupling between poles, a low height active patch is fed by vertical poles (Fig. 3 (d)). A second patch coupled to the active patch by proximity and placed much higher over the ground plane allows a wide band operation. To support both patches three supporting poles are used. These poles are made with nylon screws and two pieces of thin PTFE hose (Fig. 3 (c)).

Finally, to compensate the inductive effect of the feeding poles a mushroom capacitor is used in the top layer of the active patch (Fig. 3 (b)).

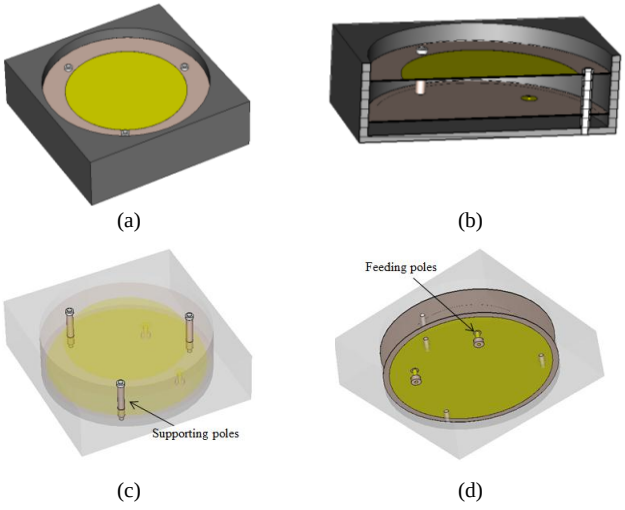

Fig. 3 Radiating element structure

III. SINGLE ELEMENT SIMULATION

The patch antenna has been analyzed using CST® software and optimized for low reflection in the working frequency band. The input impedance optimization has been done to avoid coupling between both orthogonal modes in the patch. This coupling is usually produced by the vertical poles but can be minimized choosing the adequate size of the patches.

Since the radiating element is going to work in an array grid, coupling among elements has to be taken into account. It is not possible to do the analysis of periodic structures in a triangular grid but considering a rectangular grid, the parameters obtained for periodic structures with the described design are also good.

The Simulated S-parameters for one patch using periodic boundaries are shown in Fig. 4. As it is shown the matching and the coupling between probes is below 20 dB in the working band.

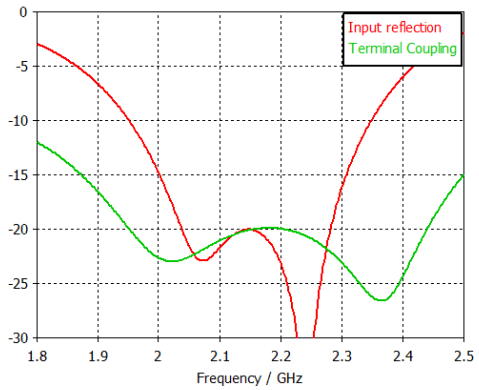

Fig. 4 Simulated S-parameters of one single patch feeding one port

To see how the mode coupling affects the input impedance, an active feeding of the patch has been done. Thus every port is fed with the same amplitude and with a phase shift of 90º for one circular polarization and with -90º for the other one. The simulated results are shown Fig. 5.

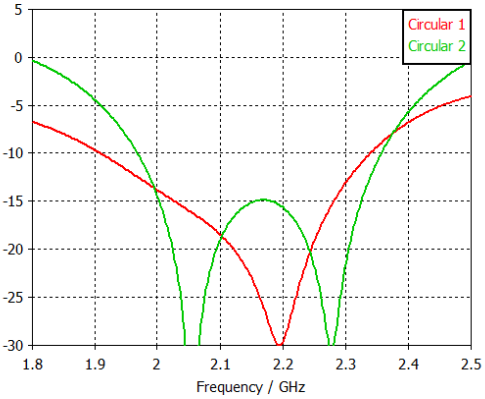

Fig. 5 Simulated S-parameters of one single patch feeding simultaneously the two ports

IV. SINGLE ELEMENT RESULTS

To check the behavior of the patch an isolated patch is manufactured (Fig. 6). To feed the patch SMP connectors have been used. We have four inputs since there are two printed couplers in a stripline below the patch for the calibration process. Therefore there are two inputs for every linear polarization and two coupled signals.

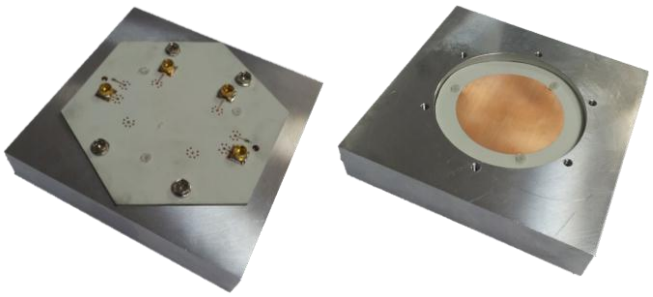

Fig. 6 Manufactured single patch

The measurements compared with the simulations are shown in Fig. 7. The matching is better than 11 dB in the working band and it is very similar to the simulation. The coupling between linear polarizations is lower than 17.5 dB. There are about 7 dB less in the measured calibration signal respect to the simulations. This should not be a big problem if it is taken into account in the calibration process. The S-Parameters of the isolated element are worse than the case of the active S-parameters of an element in the array since the optimization has been done to improve the active S-parameters of an element surrounded by elements. Therefore since there is a good agreement between the simulations and the measurements for a single element it can be concluded that the behavior of the patch in the array will be very similar to the previous simulated results.

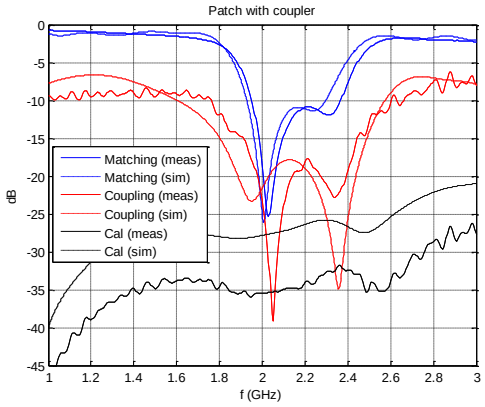

Fig. 7 Measured and simulated results of one single patch

V. CELL SIMULATION

To take into account the antenna behavior pointing to some directions, an array of several elements is analyzed. The problem is that if periodic boundaries are used the field in one edge is injected in the opposite edge. That means that the phase of the last element in the line should be equal to the phase of the element that would be before the first element. For this reason to obtain accurate results in terms of S-parameters the array of Fig. 8 is simulated. With 3x2 elements we can simulate broadside and the steering direction of a phase shift of 360/3 º that is 37º, close to the maximum steering direction of GEODA-SARAS that is 40º.

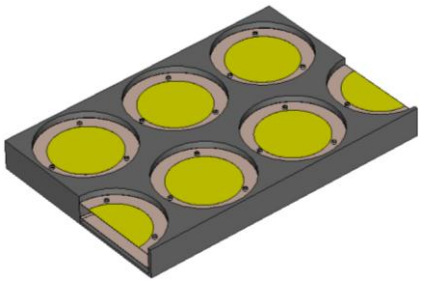

Fig. 8 Six element array with periodic boundaries

The active S-parameters for both polarizations for broadside direction are shown in Fig. 9. Since we are simulating a perfect periodic structure radiating to broadside, the S-parameters of every patch are the same. In this case we can check that the simulations of a patch in a triangular grid and in a square grid (Fig. 5) are very similar.

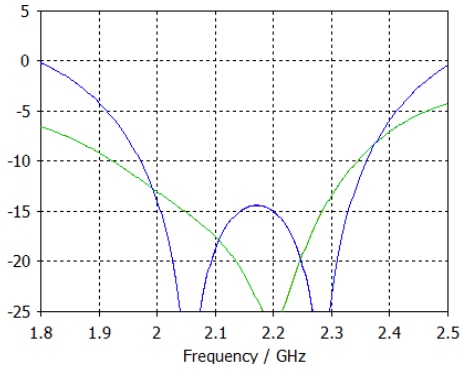

Fig. 9 Active S-parameters of the six element array for broadside direction

The active S-parameters for the antenna pointing to 37º are shown in Fig. 10. The parameters are below 10 dB in the working band.

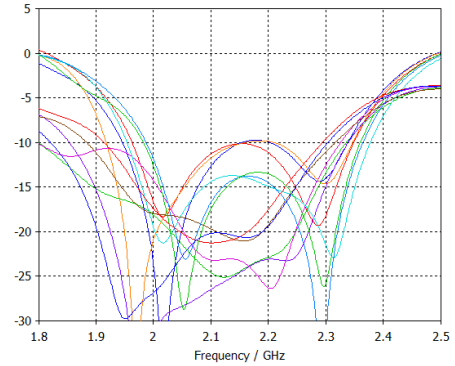

Fig. 10 Active S-parameters of the six element array steering at 37º in elevation

VI. MANUFACTURED CELL

Two cells have been manufactured to check the coupling among elements and the polarization purity. One of these cells has sequential rotation to improve the axial ratio. In Fig. 11 it can be seen the manufactured cell without the cavity.

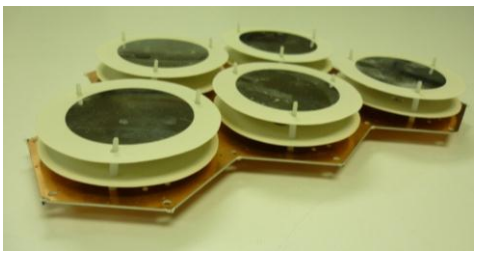

Fig. 11 Manufactured cell outside the cavity

In Fig. 12 is shown the couplings to one of the probes of the central patch. As it is seen all the coupled signals are below 16 dB in the band.

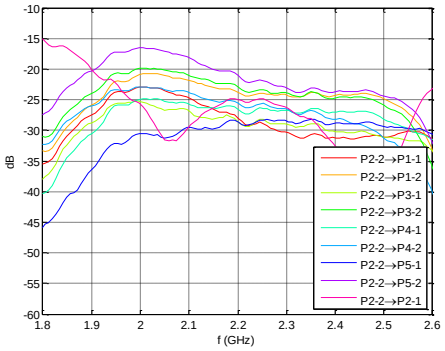

Fig. 12 Coupling to the central patch

The measured axial ratio for a cell with sequential rotation technique and for a cell without sequential rotation technique is shown in Fig. 13. Obviously the axial ratio is much better for the cell with sequential rotation technique but the RF circuit layout is more complex to design because of the rotation.

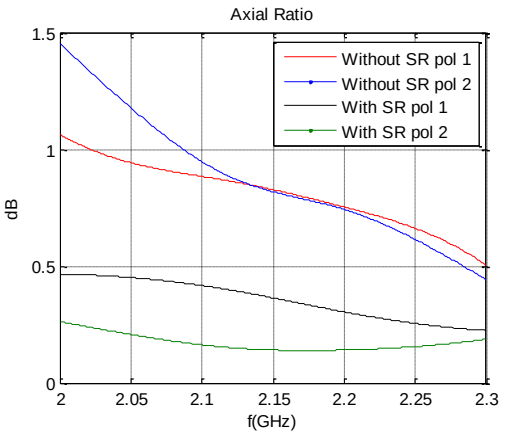

Fig. 13 Measured axial ratios without and with Sequential Rotation

VII. DIFFERENT AMPLITUDE PROBE FEEDING

The axial ratio degradation when the antenna is pointing to directions with low elevation angle is a great concern. In the case of GEODA-SARAS the axial ratio reaches 3.5 dB.

To improve the circular polarization purity the two patch probes can be fed with different amplitude signals. In Fig. 14 it is shown how the axial ratio varies when the feed amplitude ratio changes.

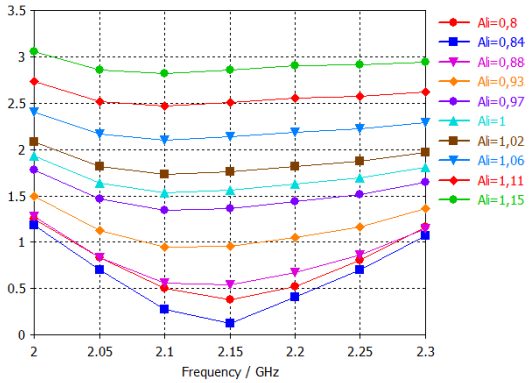

Fig. 14 Axial ratios for one patch in broadside direction changing the feed amplitude ratio

The problem is that what improves one polarization makes worse the other one. For this reason the scheme of Fig. 15 is used in the RF circuits. This way the probe ratio for each polarization in RX can be changed independently.

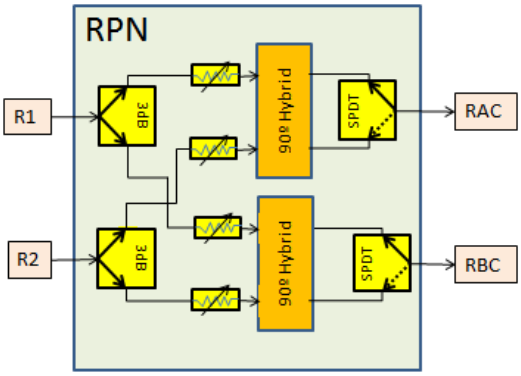

Fig. 15 Rx polarization network

VIII. AXIAL RATIO MAPS

It is possible to calculate the radiated field by one panel combining the simulated radiated field of one element with periodic boundaries. To check the behavior when the antenna is pointing, the phase of every element can be changed. This way the axial ratio can be calculated for every steering direction.

A map for the best probe ratio for the antenna pointing to every elevation an azimuth angle can be seen in Fig. 16. The azimuth directions where probe ratio changes, are related with the nulls of the patch radiation pattern.

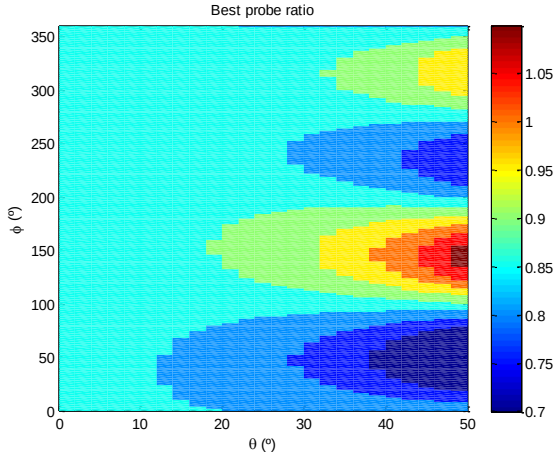

Fig. 16 Best probe ratio for every direction

In Fig. 17 is shown the best axial ratio that can be achieved changing the probe ratio according to Fig. 16. Since the maximum θ angle for the GEODA-SARAs is 40º, the axial ratio is below 1.5 dB.

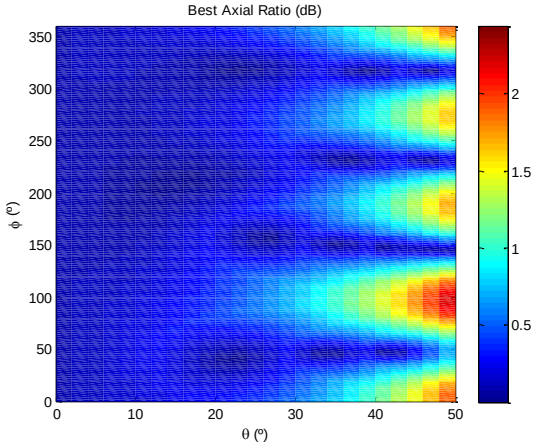

Fig. 17 Best axial ratio achieved for every direction

To calibrate the axial ratio for the real antenna a measurement of the radiation pattern for every element and for each probe in the element is needed.

IX. CONCLUSIONS

The design and measurements of the radiating element of the GEODA-SARAS project have been shown. A method to improve the axial ratio when the array is pointing to directions far from broadside has been explained. The measurements of one panel will be shown in URSI 2013.

ACKNOWLEDGMENT

Simulations done in this work have been realized using CST Microwave Studio Suite 2012 under a cooperation agreement between Computer Simulation Technology (CST) and Technical University of Madrid. The project is supported by Spanish Education Ministry (Comisión Interministerial de Ciencia y Tecnología) under reference TEC2011-28789-C02- 02, and by an UPM grant.

REFERENCES

[1] I. Montesinos, M. Sierra, J. L. Fernández, J. López, J.L. Masa, "Geoda: distribución de la celda unitaria, composición de los arrays y funcionamiento" *Simposium Nacional URSI*, Madrid, Septiembre 2008.

[2] Javier García-Gasco Trujillo , Marta Arias Campo, Ignacio Montesinos Ortego, Manuel Sierra Pérez, "Diseño del módulo T/R de la antena GEODA-GRUA", *Simposium Nacional URSI*, Bilbao, Septiembre 2010.